

Orientation of cyanine fluorophores terminally attached to DNA via long, flexible tethers

Jonathan Ouellet, Stephanie Schorr, Asif Iqbal, Timothy J. Wilson, and David M. J. Lilley

Supplementary Information

DNA sequences used to construct the duplex series

10bp

Cy3-5'-CCTAGAGTGG-3'

Cy5-5'-CCACTCTAGG-3'

11bp

Cy3-5'-CCTAGCAGTGG-3'

Cy5-5'-CCACTGCTAGG-3'

12bp

Cy3-5'-CCTAGCCAGTGG-3'

Cy5-5'-CCACTGGCTAGG-3'

13bp

Cy3-5'-CCTAGCGCAGTGG-3'

Cy5-5'-CCACTGCGCTAGG-3'

14bp

Cy3-5'-CCTAGCAGCAGTGG-3'

Cy5-5'-CCACTGCTGCTAGG-3'

15bp

Cy3-5'-CCTAGCAGGCAGTGG-3'

Cy5-5'-CCACTGCCTGCTAGG-3'

16bp

Cy3-5'-CCTAGCAGTGCAGTGG-3'

Cy5-5'-CCACTGCACTGCTAGG-3'

17bp

Cy3-5'-CCTAGCAGGTGCAGTGG-3'

Cy5-5'-CCACTGCACCTGCTAGG-3'

18bp

Cy3-5'-CCTAGCAGCGTGCAGTGG-3'

Cy5-5'-CCACTGCACGCTGCTAGG-3'

19bp

Cy3-5'-CCTAGCAGCGGTGCAGTGG-3'

Cy5-5'-CCACTGCACCGCTGCTAGG-3'

20bp

Cy3-5'-CCTAGCAGCGAGTGCAGTGG-3'

Cy5-5'-CCACTGCACTCGCTGCTAGG-3'

22bp

Cy3-5'-CCTAGCAGCGGCAGTGCAGTGG-3'

Cy5-5'-CCACTGCACTGCCGCTGCTAGG-3'

24bp

Cy3-5'-CCTAGCAGCGCAGCAGTGCAGTGG-3'

Cy5-5'-CCACTGCACTGCTGCGCTGCTAGG-3'

Purification of DNA duplexes 5'-labelled with L13-sCy3 and L13-sCy5

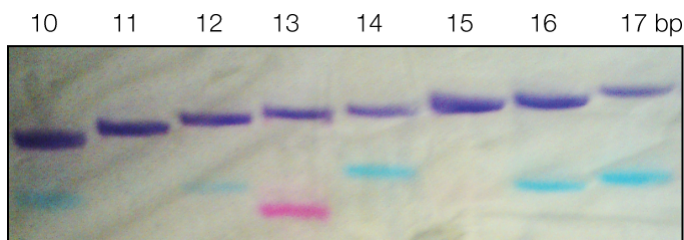


Figure S1 : Electrophoretic separation of 10 - 17 bp duplex species following hybridization. The L13-sCy3, L13-sCy5 labelled duplexes migrate as purple bands, well separated from unhybridized strands labeled with L13-sCy3 (pink) or L13-sCy5 (blue). The duplex-containing bands were excised and the DNA recovered by electroelution.

Correction of FRET efficiencies measured by single-molecule methods

Fluorescence intensities from single-molecule experiments have an inherent background. The background of the donor and the acceptor for each data acquisition was determined with a dual histogram of donor and acceptor intensities (Figure S2). Intensities of donor plus acceptor pairs, and those with donor only were fitted by linear regression and the intersection determined. The intersection of these two lines provides a measure of the background to be removed from each channel.

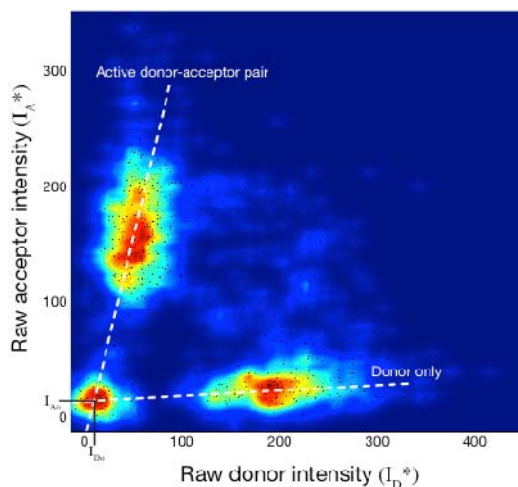


Figure S2 : Dual histogram of donor and acceptor intensities from 3532 molecules of the 10 base-pair duplex.

The background-corrected FRET efficiency (E_{FRET}^*) for a molecule, averaged over n frames (typically $n=11$), is given by :

where I_D^* and I_A^* are the raw recorded intensities and I_{D0} and I_{A0} are the background intensities of the donor and acceptor channels respectively. The gamma factor (γ) is a function of fluorophore quantum yields and photon detection efficiencies and varies

with conditions (such as pH, temperature, optical alignment and properties of optics and filters) (1). γ is calculated from the change in intensity in the donor and acceptor channels following an acceptor photobleaching (or blinking) event according to :

$$\gamma = \frac{\overline{\Delta I_A}}{\overline{\Delta I_D}}$$

where the corrected donor and acceptor intensities were averaged over a stable number of frames on either side of the photobleaching event. A total of 159 molecules (within duplexes 10 to 16) presenting these events were identified, yielding a mean value for γ of 1.162 with a 95% confidence interval of ± 0.032 .

The E^*_{FRET} population histogram usually contains two main peaks, with the peak at lower E^*_{FRET} arising from donor-only molecules with an inactive acceptor. Donor-only molecules have a non-zero E^*_{FRET} because of leakage of donor light into the acceptor channel due to the long-pass 645-nm dichroic mirror. A Gaussian fit of the E^*_{FRET} histogram allows measurement of the crosstalk correction factor p for each duplex (Figure S3).

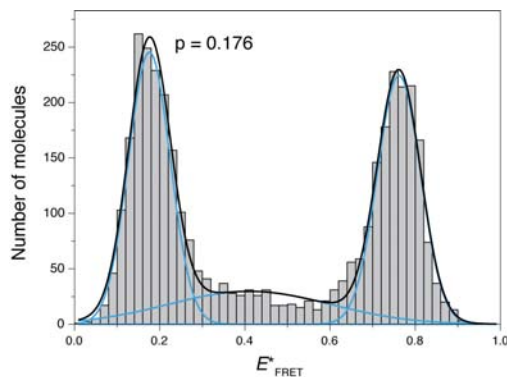


Figure S3 : Background-corrected FRET efficiencies histogram from 3532 molecules of the 10 base-pair duplex. The histogram was fitted to three Gaussian functions to determine the donor-only peak position p .

A further correction is required because of reflection of acceptor light into the donor channel by the 645-nm dichroic mirror. The backreflection ratio r was measured with a dual-labelled DNA hairpin (Figure S4) where the donor and acceptor are so close that $E_{\text{FRET}} \approx 1$ so that all the emission arises from the acceptor. We measured $E^*_{\text{FRET}} = 0.967$, thus $r = 0.037$.



Figure S4 : Sequence of a DNA hairpin loop with a two base-pair separation of donor and acceptor to measure the back-reflection correction factor r .

The true FRET efficiency for each molecule is given by :

$$E_{FRET} = \frac{E_{FRET}^* - p}{1 - r - p}$$

The E_{FRET} population histogram fitted to multiple Gaussian functions (Figure S5), provides the best estimate of the FRET efficiency for a particular DNA duplex.

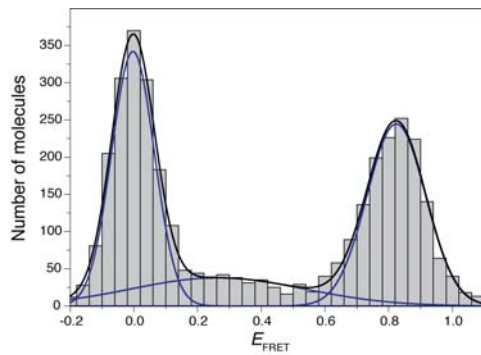


Figure S5 : Background, crosstalk and backreflection-corrected FRET efficiencies histogram of the 10 base-pair duplex fitted to three Gaussian functions.

The uncertainty associated with each E_{FRET} value was calculated using the uncertainties of the fitted parameters and the estimated errors of the correction factors. It was assumed that the background intensities I_{D0} and I_{A0} have a negligible error. The 95% confidence interval of ± 0.032 for γ was used to calculate upper and lower limits for E_{FRET}^* . For example, the background-corrected data for the 10 base-pair duplex gave $E_{FRET}^* = 0.811$ and 0.803 using the lower and upper values of γ respectively, giving $E_{FRET}^* = 0.807 \pm 0.004$.

The error in the crosstalk correction factor p was also calculated using the upper and lower boundaries of γ . For the 10 base-pair duplex p varied between 0.109 to 0.103 for the lower and upper γ respectively (95% confidence interval), giving $p = 0.106 \pm 0.003$. The standard deviation from the Gaussian fit used to determine the back reflection correction factor was used to estimate the uncertainty in r , resulting in $r = 0.037 \pm 0.004$. The overall uncertainty in E_{FRET} was calculated as :

$$\Delta E_{FRET} = \sqrt{\left(\frac{\Delta E_{FRET}^* + \Delta p}{E_{FRET}^* - p}\right)^2 + \left(\frac{\Delta r + \Delta p}{1 - r - p}\right)^2} \cdot E_{FRET}$$

The 10 base-pair DNA duplex is then found to have $E_{\text{FRET}} = 0.824 \pm 0.010$. The same procedure was applied for all 13 DNA duplexes, and the resulting histograms are presented in Figure S6.

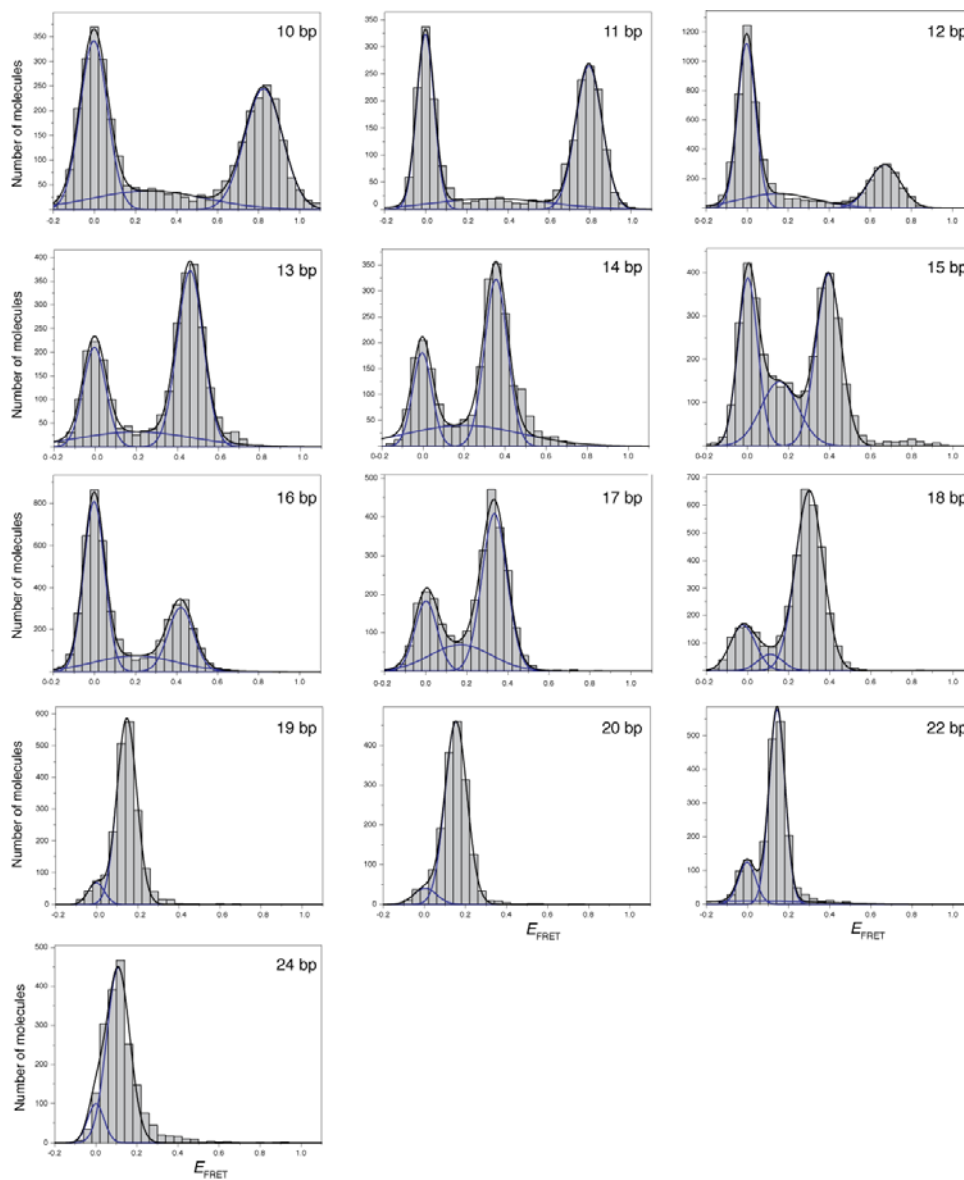


Figure S6 : Histograms of corrected FRET efficiency for each member of the DNA duplex series.

Modelling the dependence of FRET efficiency on duplex length with lateral mobility of fluorophores

This is calculated as presented in Iqbal et al (2). We calculate the interfluorophore distance for each duplex R as

$$R = ((L-1) \times H) + D$$

where L is the length of the helix (bp), H is the helical rise per bp step, and D is the additional axial separation for the two fluorophores.

The mean angle between the transition moments A is calculated as :

$$A = ((L-1) \times T) + C3A + C5A$$

where T is the twist angle for each basepair, and $C3A$ and $C5A$ are the rotations of Cy3 and Cy5 relative to the terminal basepairs. For B form DNA $H = 3.6 \text{ \AA}$ and $T = 36^\circ$, and $D = 8 \text{ \AA}$. $C3A + C5A = 62^\circ$ for the L3-Cy3 plus L3-Cy5 combination, and 0° for the L13-sCy3 plus L13-sCy5 combination.

For each species, we set up an array of angles (AA) over a $\pm 100^\circ$ range about the mean. κ^2 and hence R_0 are calculated for each length. The value of E_{FRET} is calculated for each angular position (E_{AA}), and the resulting distribution summed, weighted by its distance from the mean angle using a Gaussian distribution, i.e.

$$E_{FRET} = \sum (E_{AA} \times P) \quad \text{where } P = \exp(-AA^2 / 1.44H^2)$$

where H is the half-width. The sum of P is normalised to unity.

This simulation procedure has been implemented in a MATLAB program.

A simulation based on fully-stacked fluorophores is presented in Figure S7.

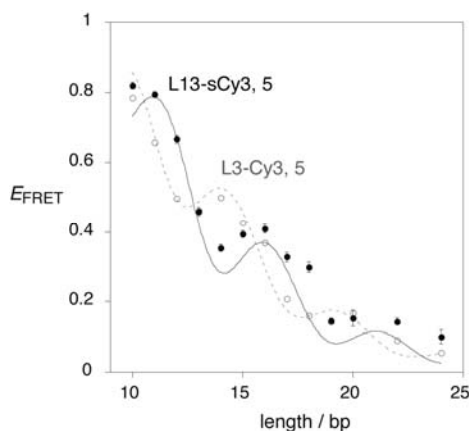


Figure S7 : Variation of FRET efficiency between L13-sCy3 and L13-sCy5 terminally attached to DNA as a function of helix length measured in phospholipid vesicle-encapsulated single molecules. The E_{FRET} values are plotted (solid circles) as a function of helix length, with estimated errors. The data have been simulated (black line) using a model in which 100% of the molecules had both fluorophores terminally stacked. The best fit was obtained where there was 0° mean rotation of each fluorophore relative to the terminal basepair. However, lateral rotation of the fluorophores was permitted about the mean, with a half-width of 45° . Standard B-form geometry of the DNA helix was used, with 10.5 bp/turn and a helical rise of $3.6 \text{ \AA}/\text{bp}$ step. These calculations were based upon a measured value of the spectral overlap integral $J(\lambda) = 5.4 \times 10^{-13} \text{ M}^{-1} \text{ cm}^3$, refractive index $n = 1.33$ and a quantum yield for L13-sCy3 of $\phi_D = 0.35$. The data (open circles) and simulation (broken line) for a duplex series with

L3-Cy3 and L3-Cy5 are plotted, taken from our earlier study (2). In this simulation the mean position of each fluorophore is rotated by 31° relative to the terminal basepair.

Modelling the dependence of FRET efficiency on duplex length with lateral mobility of fluorophores, together with an unstacked fraction

Where a fraction of unstacked fluorophores is allowed, the value of E_{FRET} for that fraction is calculated using $\kappa^2 = 2/3$, together with an increment to the interfluorophore distance. The resulting E_{FRET} is calculated as a linear combination of the contributions from the stacked fluorophore (calculated as described in the preceding section) and the freely-mobile fluorophore. This simulation procedure has been implemented in a MATLAB program.

Calculation of Förster length R_0 for L13-sCy3 and L13-sCy5 attached to double-stranded DNA as NHS esters.

The overlap integral $J(\lambda)$ has been evaluated over the wavelength range 520-700 nm. An absorbance spectrum of a DNA duplex containing a sCy5 dye conjugated as NHS ester attached to one of the strands was recorded. Additionally, a fluorescence spectrum of a DNA duplex containing a sCy3 dye conjugated as an NHS ester attached to one of the strands was recorded.

The L13-sCy5 duplex absorption was scaled to the molar absorbance of the sCy5 NHS ester of 250,000 at a wavelength of 651 nm. The overlap integral was evaluated numerically from these spectra, normalized to the sCy3 fluorescence over the same range, according to:

$$J(\lambda) = \frac{\sum \text{Fluorescence}(\text{sCy3}) \times \text{Absorbance}(\text{sCy5}) \times \lambda^4}{\sum \text{Fluorescence}(\text{sCy3})}$$

$$= 5.421 \times 10^{-13} \text{ M}^{-1} \text{ cm}^3$$

The Förster length R_0 can be calculated from :

$$R_0^6 = \frac{0.529 \times \kappa^2 \times \phi_D \times J(\lambda)}{N \times n^4}$$

$$R_0 = 5.70 \times 10^{-7} \text{ cm} = 57 \text{ \AA}$$

where $\kappa^2 = 2/3$ and the quantum yield of the donor $\phi_D = 0.35$, the Avogadro number N and the refractive index of water $n = 1.33$.

Fluorescent lifetime decay for L13-sCy3 and L3-Cy3 5'-attached to DNA as a function of terminal sequence.

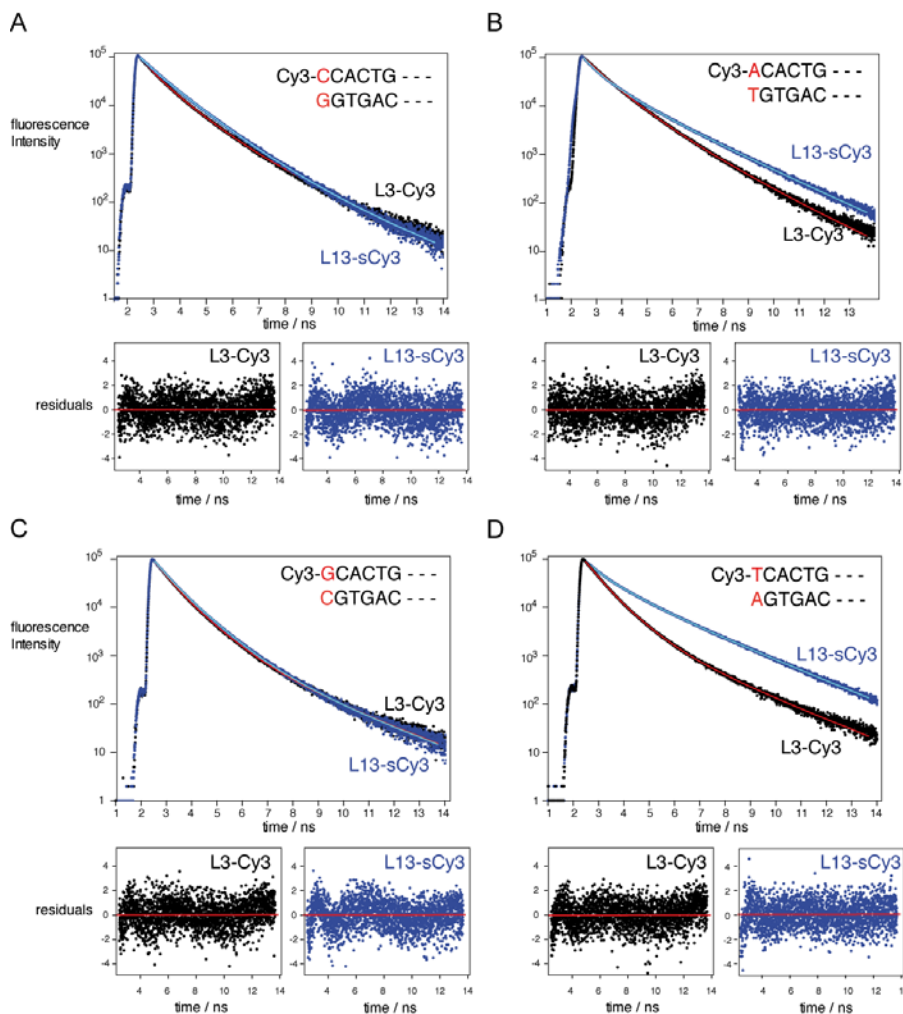


Figure S8 : Time-resolved fluorescence decay of L13-sCy3 and L3-Cy3 terminally attached to DNA as a function of the sequence of the terminal basepair. 16 bp duplexes based on the sequence Cy3-**X**CACTGCACTGCTAGG where **X** is C (panel A), A (panel B), G (panel C) and T (panel D) were studied. In each case the decay curves and fits are shown in the larger panels, with the residuals for the fits shown below. L13-sCy3 data are shown in blue (fits shown blue), L3-Cy3 data in black (fits shown red). The lifetimes calculated from these data are presented in Table 1.

Synthesis of Cy3 phosphate for fluorescence lifetime measurements

Cy3 phosphate (Figure S9) was synthesised using standard CE-phosphoramidite chemistry on an automated DNA synthesiser. A phosphorylation reagent (2101-F100, Link Technologies) was first coupled to a standard preloaded DNA synthesis column (universal support) followed by the Cy3 phosphoramidite (28-9172-98, GE Healthcare). The Cy3 phosphate was cleaved from the solid support and the CE protecting group removed by treatment with concentrated ammonium hydroxide solution (Fisher) then dried in vacuo.

Purification was then by reversed-phase HPLC (Buffer A: 0.1 M TEAA pH 7.0 Buffer B MeCN, 1 mL min⁻¹, 1-5 min 100% A, 5-12 min 80% A, 12-32 min 70% A, 32-37 min 55% A, elution at 36 min). ESI-MS negative mod [C₂₉H₃₆N₂O₅P]: calculated 523 Da, found 523 Da.

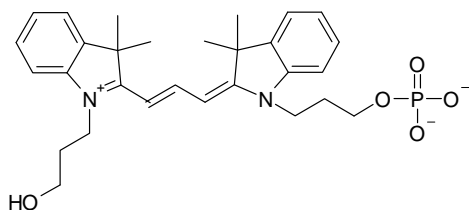


Figure S9 : The structure of Cy3 phosphate used in fluorescence lifetime measurements.

References

1. Lee, N. K., A. N.Kapanidis, Y. Wang, X. Michalet, J. Mukhopadhyay, R. H. Ebright, &S. Weiss (2005) *Biophys. J.* 88: 2939-2953.
2. Iqbal, A., S. Arslan, B. Okumus, T. J.Wilson, G. Giraud, D. G. Norman, T. Ha &D. M. J. Lilley (2008) *Proc. Natl. Acad. Sci. USA* 105: 11176-11181.